
Enhancing Urban Wireless Networks with Modular Reflecting EM Skins

P. Rocca, P. Da Rù, N. Anselmi, M. Salucci, G. Oliveri, and A. Massa

2024/07/05

Contents

1 Smart Environment Simulation	3
1.1 Principles and Setup	3
1.2 Surface influence analysis	5
1.2.1 Smart skin radiating towards a single point	7
1.2.2 Smart skin radiating towards distributed points	9
1.2.3 Additional comments and comparison	11
1.2.4 Effect of phase term ϕ_{ref}	12
1.3 The Optimization	14
1.3.1 The NSGA-II algorithm	15
1.3.2 Cost function definition	15

1 Smart Environment Simulation

The final step of the presented research activity involves the definition of a complete scenario in which to test the developed software and its integration with a multi-objective optimizer to handle the trade-off between the quality of the signal at the receiver and the complexity of the smart skin deployment. The chosen implementation scenario is a medium density small city, with an average building height lower than 20 [m], an hypothetical transmitting basestation on the roof of one building, and receivers scattered in a blind spot area at a general user device height of 1.5 [m] from the ground.

1.1 Principles and Setup

A smart electromagnetic skin is a device composed of dozens of small passive metasurfaces embedded in the external wall of a building, and coordinated to radiate an impinging signal towards one or multiple points inside a region where the coverage would otherwise be lackluster.

To allow for the correct modelling of a smart skin placed on the facade of a building, the original code had to be adapted in order to rotate the coordinate system and have the base metasurface modelled vertically. Given the “old” cartesian reference system (x, y, z) , in which the coordinates for the correct computation of the formulas are defined, and the “new” one (x', y', z') , which describes the scenario coordinates, a simple transformation was performed in order to align the two regimes and maintain the correct working of the surface while allowing a more natural and immediate definition of the communication scenario. A visual representation of the transformation has been reported in Figure 1, where the new meaning of the angles θ and φ , as a result of the redefinition of the system’s axes can be seen.

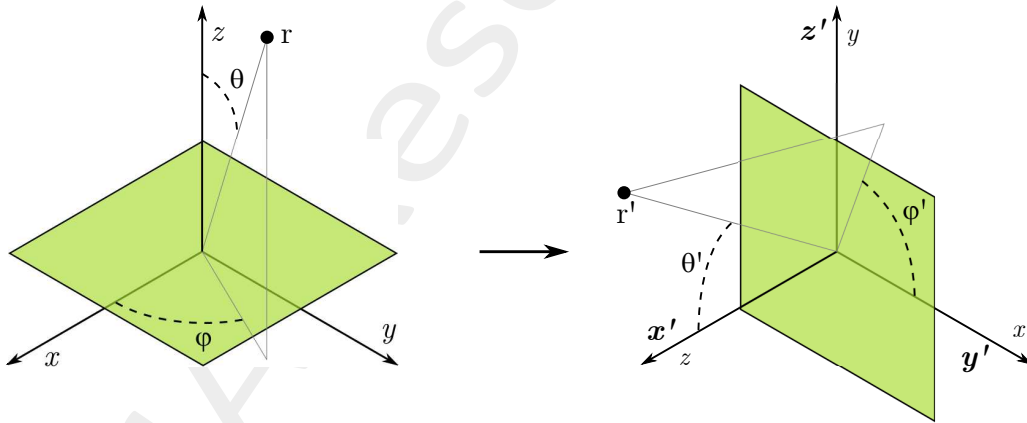


Figure 1: Change of the reference system from the “horizontal surface” - in which the angles θ and φ are computed for the formulas - to the “vertical surface” - in which the scenario coordinates are defined.

The code was then expanded with a consideration of multiple vertical surfaces, each one radiating toward a specific desired point, and with multiple observer points also placed at specified coordinates inside the area of interest, to take into consideration many different end-user devices inside the blind area, for which the optimizer would try to obtain the best coverage during the final optimization step.

To analyze the correct functioning of the smart skin in the new reference system, a series of tests has been performed, considering different positions of the target point towards which the smart skin was set to radiate. Four of the basic validation tests considered are schematized in Figure 2

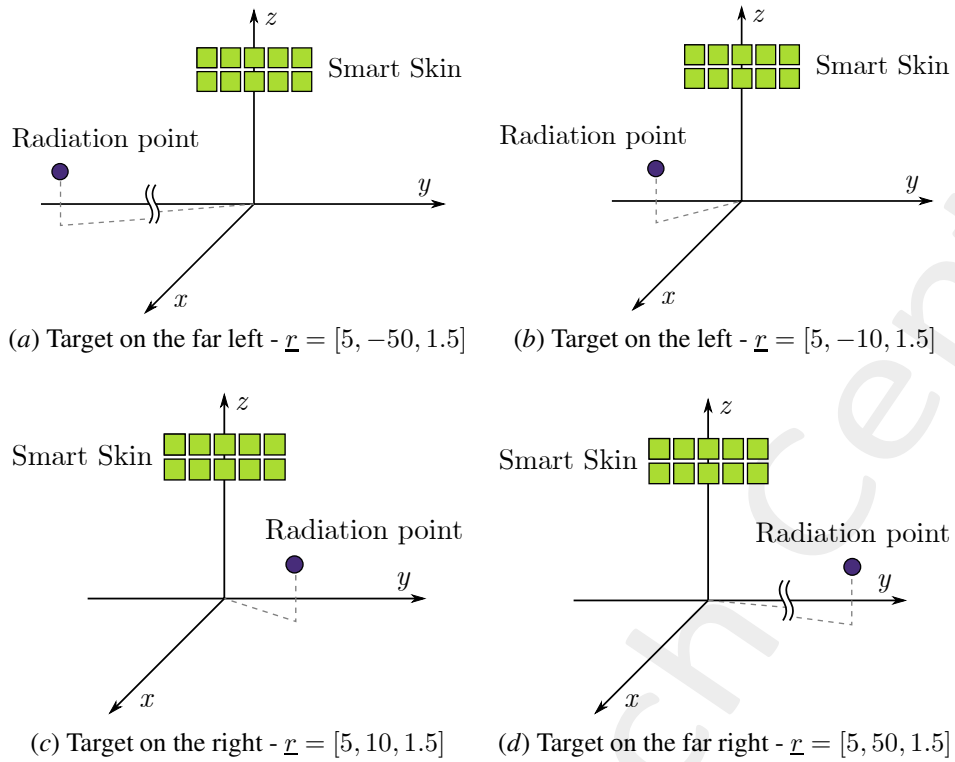


Figure 2: Four main test cases for the validation of the vertical smart skin.

As can be easily understood, the four main cases consider the target point of the radiation in front of the smart skin, at a fixed distance of 5 [m] along the x -axis and four distances along the y -axis: -50, -10, 10 and 50 [m]. The target is always considered at a user height of 1.5 [m].

In the following Figure 3 the resulting heatmaps for the electric field $F_R(\underline{r})$ are reported, where it is clear how the field is correctly directed toward the expected direction.

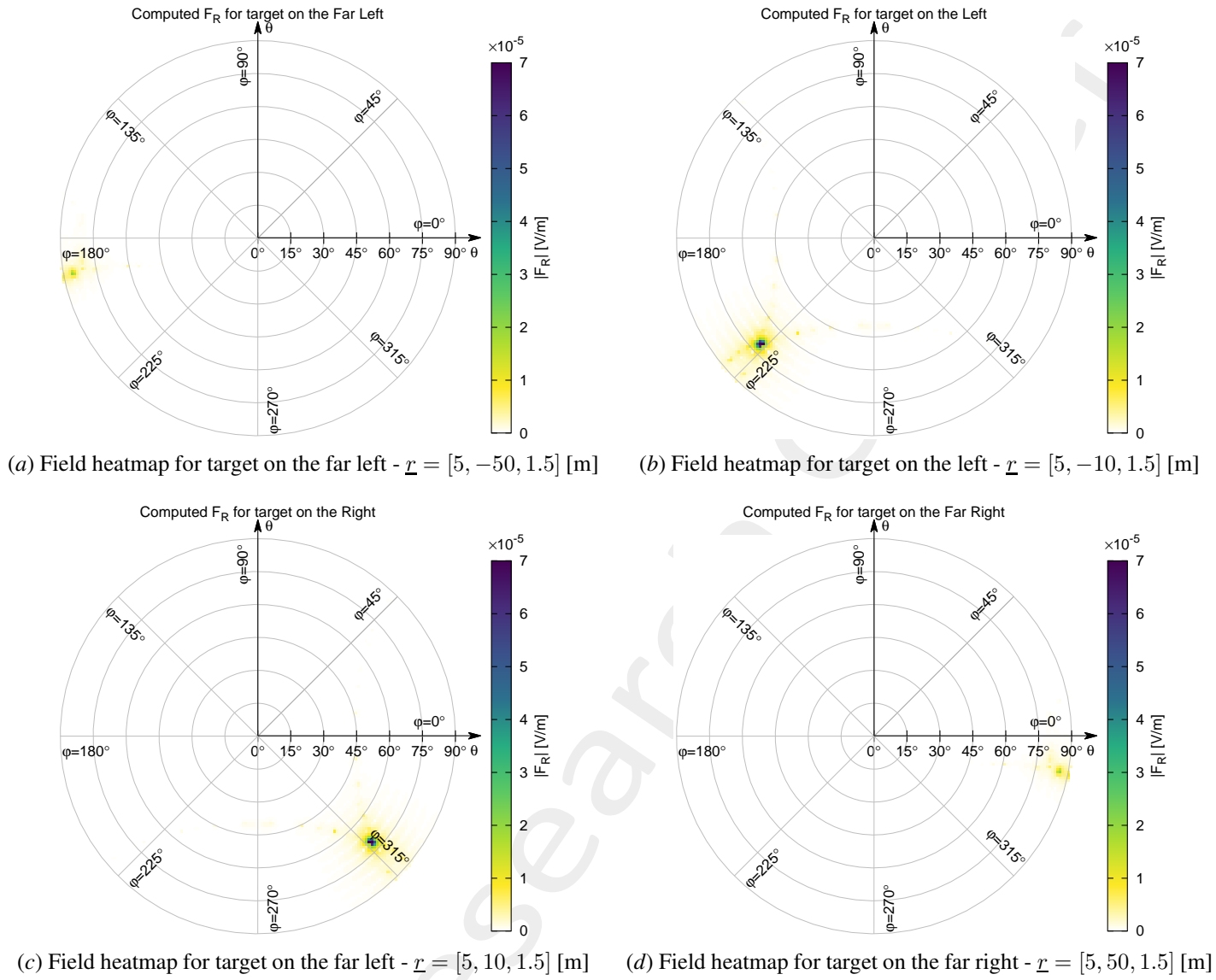


Figure 3: Polar heatmaps of the vertical smart skin for four different radiation directions - target closing in from the left and leaving from the right.

1.2 Surface influence analysis

As the principles of the system were proven valid and correctly working, a series of simulations has been conducted to assess the effects that each of the surfaces or a combination thereof would produce on the final distribution of field. A simple scenario was defined, with a matrix of 2×5 metasurfaces considered for the smart skin, in a scenario having the following characteristics:

- The reference system was considered centered on the ground below the first column of metasurfaces, with the smart skin developing on the y - z plane and the x -axis orthogonal to the plane itself;
- The single metasurface is square, with dimension 0.5×0.5 [m];
- The smart skin was divided into two rows and two columns of metasurfaces, with coordinates:
 - $x = 0$ [m] for all surfaces

- $y = [0; 0.5; 1; 1.5; 2]$ [m]

- $z = [7.5; 8]$ [m]

- The transmitting base station was considered at a distance of 300 [m] from the smart skin, and at a plausible height of 25 [m], as a standard for a urban scenario in 5G communications;
- The area of interest (AoI), or blind spot, was defined as an area 10×50 [m] at a distance of 200 [m] from the smart skin;
- The relevant coordinates of the system are resumed in Table I.

Table I: Relevant coordinates of the system for the early smart skin analysis

	x [m]	y [m]	z [m]
Base Station	300	0	25
AoI center	5	200	1.5
AoI closest corner	0	175	1.5
AoI farthest corner	10	225	1.5
First surface center	0	0	8
Spatial shift of additional surfaces	~	+0.5	+0.5

In this scenario, two main cases were defined and simulated, and are thoroughly analyzed in the following subsections:

1. All the metasurfaces on the smart skin radiating towards the same direction, the center of the AoI $\underline{r} = [5, 200, 1.5]$;
2. Ten radiation points defined inside the AoI, each one used as the radiation target by one of the metasurfaces.

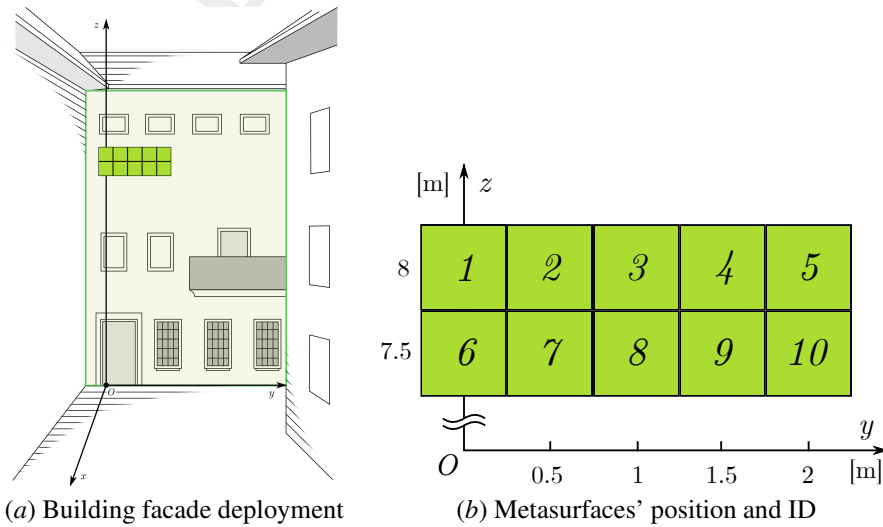


Figure 4: Building facade and numbering of the metasurfaces for the early smart skin analysis

1.2.1 Smart skin radiating towards a single point

This case considers a situation in which all the metasurfaces are set to reflect the incoming field towards the same point \underline{r} , at the center of the AoI. In this case the maximum field power obtainable is expected in \underline{r} , as all the metasurface radiate the power impinging on the smart skin towards a single point; from this point of view, the working regime can be considered as a perfect focusing of the entire smart skin considered as a single device (it is however important to specify that the single metasurfaces that compose the smart skin always work in the “anomalous reflection” regime).

In Figure 5 some of the considered cases are presented, whereas Table II contains the numerical values for these test cases. As can be deduced from the data and from the plots, there is little to no difference in the signal strength coming from the singular individual surfaces, be it maximum or average, with a slight advantage for those deployed closer to the AoI. Interestingly, it can be noticed how the compensation of the phase delay $\Delta\phi$ allows for an almost perfect constructive interference of the metasurfaces contributions, and how therefore the case with two radiating surfaces manifests a field twice as strong as the one with a single one, and how the case with all ten transmitting increases the received field strength tenfold.

Table II: Relevant electromagnetic quantities for the single smart skin radiation point - AoI center at $\underline{r} = [5, 200, 1.5]$

Test case	1	2	3	4
Number of active surfaces	1	1	2	10
Active surfaces ID	1	2	1, 2	[1:10]
Reference Figure	5 (a, e)	5 (b)	5 (c)	5 (d, f)
$ F_R(\underline{r}) _{lin}$ [V/m]	1.524×10^{-5}	1.528×10^{-5}	3.052×10^{-5}	1.532×10^{-4}
$ F_R(\underline{r}) _{dB}$ [dB]	-96.34	-96.32	-90.31	-76.29
Minimum of $F_R _{lin}$ [V/m]	6.340×10^{-6}	6.284×10^{-6}	1.262×10^{-5}	6.744×10^{-5}
Minimum of $F_R _{dB}$ [dB]	-103.96	-104.04	-97.98	-83.38
Maximum of $F_R _{lin}$ [V/m]	1.535×10^{-5}	1.539×10^{-5}	3.074×10^{-5}	1.543×10^{-4}
Maximum of $F_R _{dB}$ [dB]	-96.28	-96.26	-90.25	-76.23
Average $F_R _{lin}$ [V/m]	1.261×10^{-5}	1.261×10^{-5}	2.522×10^{-5}	1.280×10^{-4}
Average $F_R _{dB}$ [dB]	-97.99	-97.99	-91.97	-77.86
Variance	5.266×10^{-12}	5.385×10^{-12}	2.130×10^{-11}	4.837×10^{-10}

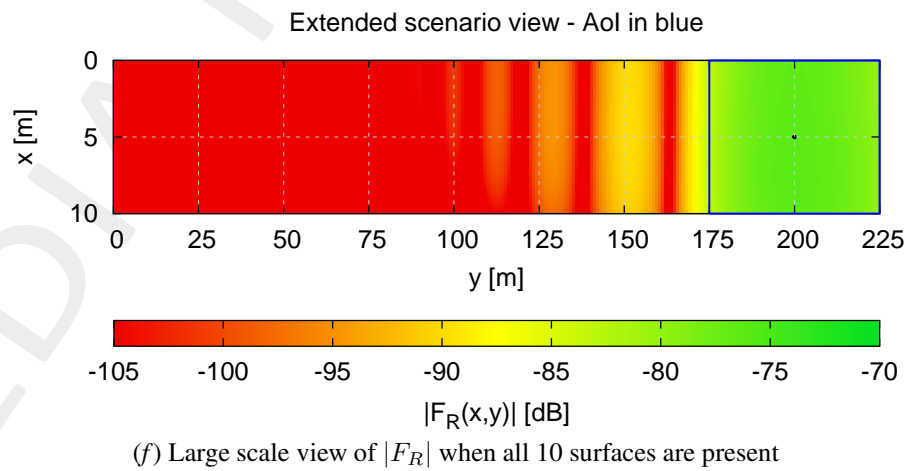
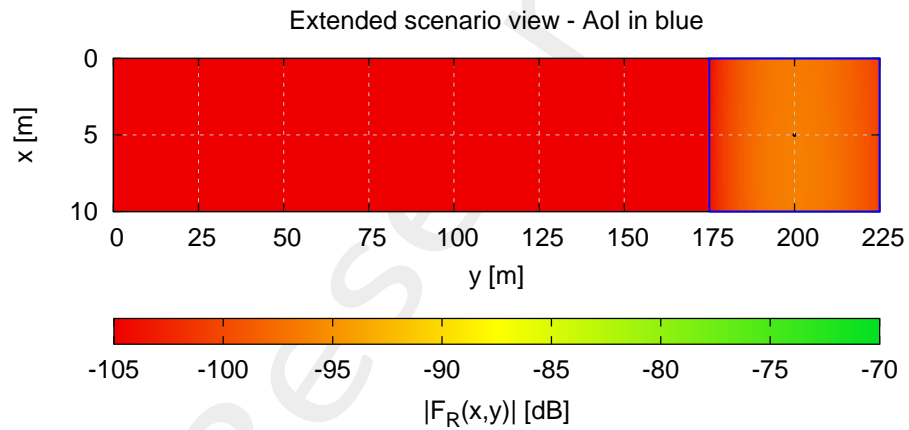
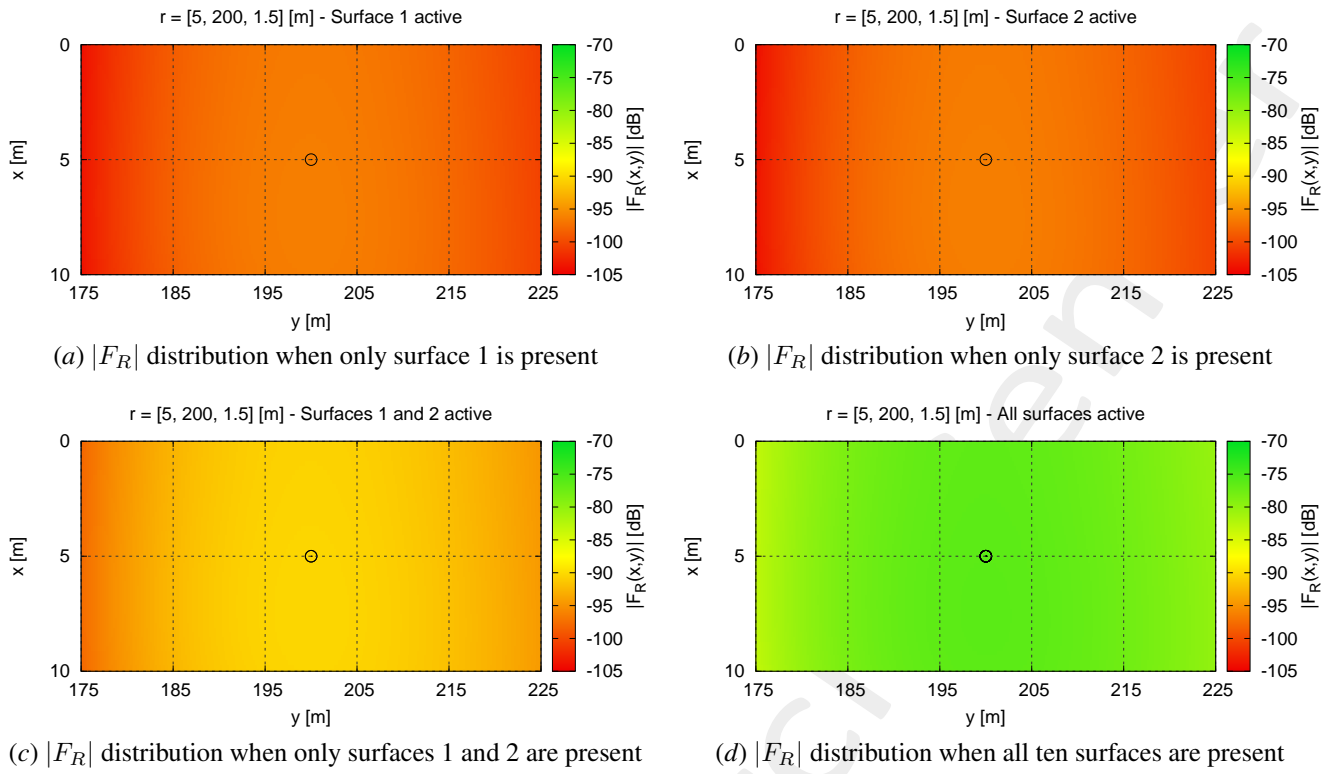


Figure 5: Smart skin with all metasurfaces radiating towards a single point $\underline{r} = [5, 200, 1.5]$

1.2.2 Smart skin radiating towards distributed points

This case considers a situation in which each one of the metasurfaces that compose the smart skin is set to reflect the incoming field towards an individual point inside the AoI. The choice of the position of these radiation points has been made to try and distribute the reflected field in a somewhat uniform manner over the blind spot. This form of distribution of the signal can be potentially more appealing for a real-life scenario with a large area of blind spot, as the total power incoming from the smart skin can be allocated in a more adaptive manner in order to improve the system behaviour inside those zones where the coverage is more critical or where a larger number of users can be expected. The coordinates of the ten radiation points are reported in Table III.

Table III: Radiation points (x, y) coordinates for the distributed radiation of the smart skin

Surface ID	x [m]	y [m]	Surface ID	x [m]	y [m]
1	2.5	180	6	7.5	180
2	2.5	190	7	7.5	190
3	2.5	200	8	7.5	200
4	2.5	210	9	7.5	210
5	2.5	220	10	7.5	220

In Figure 6 some of the considered cases are presented, and is immediately noticeable how different surfaces correctly radiate their beam towards different directions, and again in Table IV the numerical values for these test cases are reported for a more thorough analysis. As can be deduced from the data and from the plots, the difference between the single radiating surfaces is minimal and can be related to the different positions of the radiation points. In this case, the average value for the case with all the surfaces considered appears to be larger than the expected ten times average of the singular case, and this is due to the fact that the peak of radiation is closer to the edge of the AoI, and some of the power is radiated outside of it (especially visible in Figure 6 (e) with part of the power radiated to the left of the AoI).

Table IV: Relevant electromagnetic quantities for the distributed pattern of smart skin radiation points - AoI center at $\underline{r} = [5, 200, 1.5]$

Test case	1	2	3	4
Number of active surfaces	1	1	2	10
Active surfaces ID	1	5	1, 2	[1:10]
Reference Figure	6 (a, e)	6 (b)	6 (c)	6 (d, f)
$ F_R(\underline{r}) _{lin}$ [V/m]	1.054×10^{-5}	1.016×10^{-5}	2.509×10^{-5}	1.294×10^{-4}
$ F_R(\underline{r}) _{dB}$ [dB]	-99.45	-99.86	-92.01	-77.76
Minimum of $F_R _{lin}$ [V/m]	5.971×10^{-10}	1.054×10^{-9}	3.189×10^{-11}	7.176×10^{-5}
Minimum of $F_R _{dB}$ [dB]	-184.48	-179.54	-209.93	-82.88
Maximum of $F_R _{lin}$ [V/m]	1.696×10^{-5}	1.399×10^{-5}	3.209×10^{-5}	1.309×10^{-4}
Maximum of $F_R _{dB}$ [dB]	-95.41	-97.08	-89.97	-77.66
Average $F_R _{lin}$ [V/m]	9.738×10^{-6}	8.704×10^{-6}	2.160×10^{-5}	1.112×10^{-4}
Average $F_R _{dB}$ [dB]	-100.23	-101.21	-93.31	-79.08
Variance	3.327×10^{-11}	2.300×10^{-11}	8.847×10^{-11}	2.403×10^{-10}

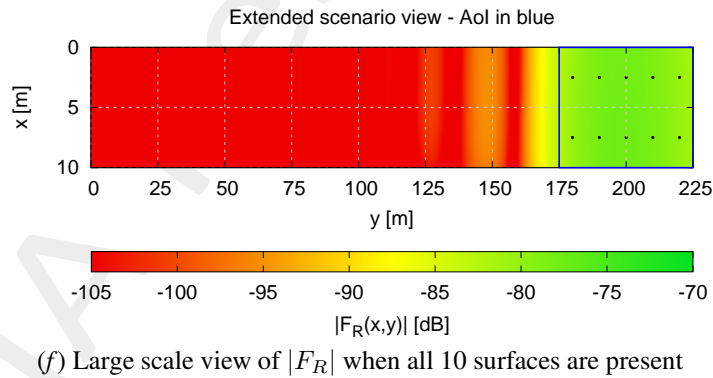
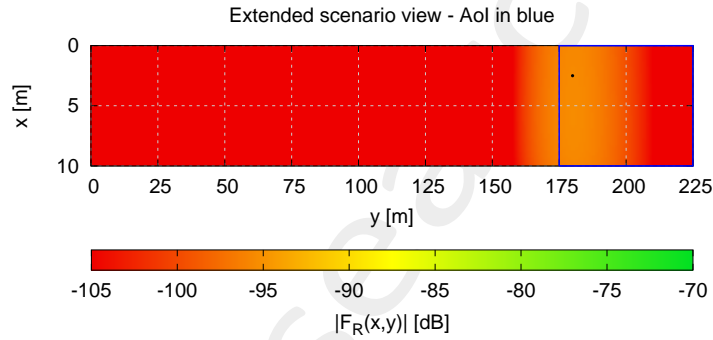
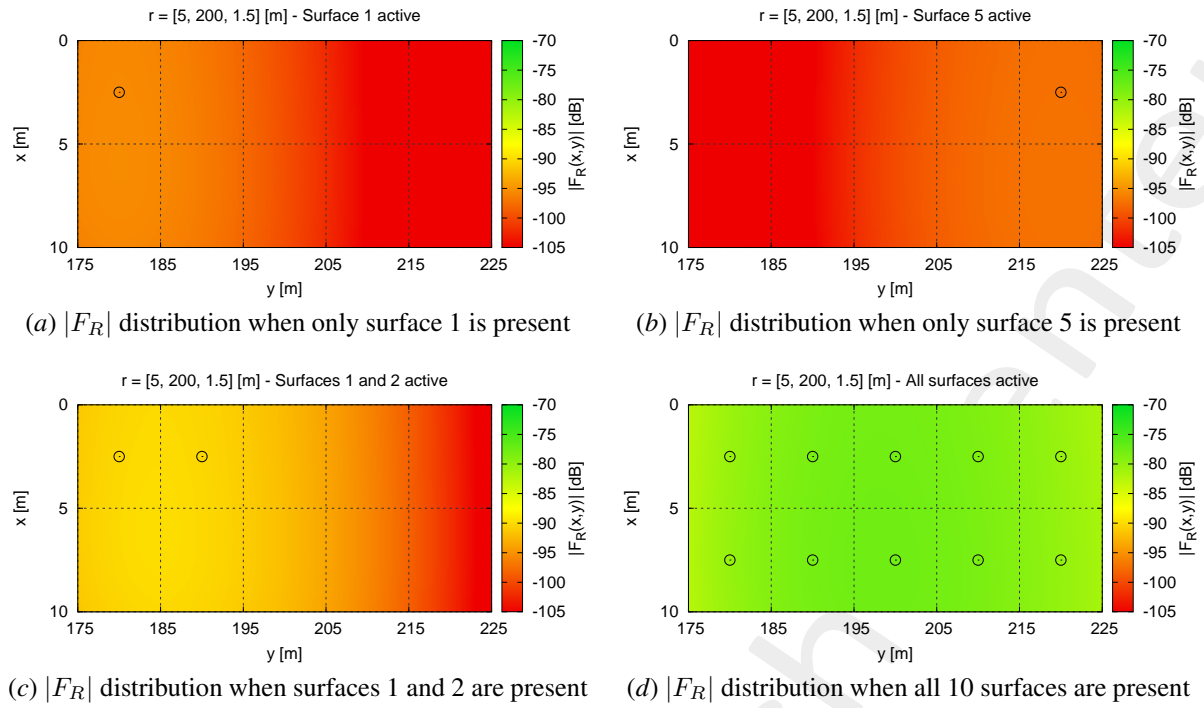


Figure 6: Smart skin with each one of the metasurfaces radiating towards a specified point inside the AoI

1.2.3 Additional comments and comparison

When comparing the two working scenarios of the previous subsections, some parallels can be drawn and some differences can be identified.

First of all, the working condition with all the surfaces present leads to similar results both for the “focused” smart skin and for the one with distributed radiation points. In this case, the few dB of average advantage of the former can be justified in part with the fact that the distributed radiation points cause part of the radiation to be “wasted” outside of the

area of interest, and in part because of the small loss of efficiency caused by the spatial differences of the various radiating points, which causes a certain degree of destructive interference which causes a partial loss of the average signal power.

The minimum value assumed for the field when all ten surfaces are present is however slightly higher for the distributed radiating regime, as can be expected by the previous reasoning. Moreover, the lower limit of the field, i.e., the minimum value of $|F_R|$ in the AoI tends to be different orders of magnitude lower when a single surface is considered radiating in a point close to the edge of the AoI, and can be reasonably justified with the incapability of a single surface to offer a satisfactory level of coverage to the entire blind area.

Apart from these differences, it is clear how the working conditions of the two scenarios can be considered similar in many ways, and their behaviour reflects overall what would be expected from the mathematical definitions presented in the previous chapter.

1.2.4 Effect of phase term ϕ_{ref}

In order to correctly model the multitude of small metasurfaces that compose an electromagnetic smart skin, the code was expanded to define and work with multiple reflecting surfaces instead of a single one; to achieve the maximum field possible at a given position and correctly compensate for the spatial differences of the metasurfaces, a phase correction was added through the term ϕ_{ref} in the formula describing the field F_R in order to align the single complex contributions towards the specified radiation point and maximize the total field there.

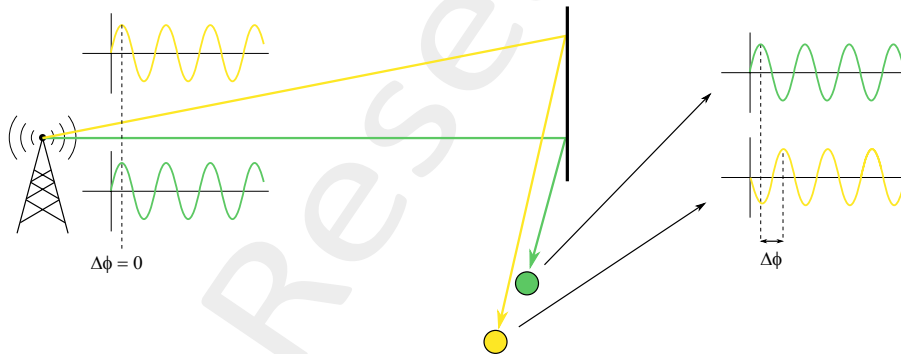


Figure 7: Schematization of the emergence of a phase delay $\Delta\phi$ due to different paths travelled by different signals

The introduction of the term ϕ_{ref} , computed dynamically for each individual metasurface, allows to take into consideration the various phase delays caused by the differences in the distances Tx-to-Surface and Surface-to-Rx that the signal has to travel. In Figure 7 a simple representation of the phenomenon is proposed, in which it is highlighted how two signals leaving the same BS at the same time (therefore with an initial phase delay $\Delta\phi = 0$) will get progressively misaligned due to different lengths of the paths they travel. The term ϕ_{ref} is therefore particularly important to counterbalance the phase delay $\Delta\phi$ and avoid that the complex field contributions coming from the different surfaces do not combine as destructive interference, virtually negating the benefit of having multiple surfaces transmitting at the same time.

The computation of the term $\phi_{ref} = \Delta\phi$ has been performed as the result of the proportion (1):

$$\Delta\phi : 2\pi = \Delta\lambda : \lambda \quad (1)$$

where $\Delta\lambda$ is the remainder of the division between the total distance travelled by the signal and the wavelength λ (2):

$$\Delta\lambda = \text{modulo} \left(\frac{r_{inc} + r_{rad}}{\lambda} \right) \quad (2)$$

$$\Delta\phi = \frac{2\pi \cdot \Delta\lambda}{\lambda} \quad (3)$$

Numerical values in Table V highlight the profound difference in the functioning of the system when the phase delay of the signal $\Delta\phi$ is not properly compensated, as the peak value of the fields between the two cases (compensated and not) drops of almost 20 [dB], and the average value drops of almost 20 [dB]. In the following Figure 8 the magnitude of the final field $|F_R|$ is reported for the case in which ten surfaces are considered, each one radiating towards a point in the AoI, marked with a black circle. It is even more clearly highlighted how the performance of the smart skin is optimal when the phase delay is compensated with a properly computed term ϕ_{ref} , and how the performance of the very same system drastically degrades when the term $\Delta\phi$ is ignored - i.e., the compensating term ϕ_{ref} is set to zero or another fixed value equal for all the metasurfaces.

Table V: Effect of the phase compensation on the electric field F_R

Test case	$\phi_{ref}(m) = \Delta\phi_m$	$\phi_{ref}(m) = 0$
Number of active surfaces	10	10
Active surfaces ID	[1:10]	[1:10]
Reference Figure	8 (a, c)	8 (b, d)
Minimum of $F_R _{lin}$ [V/m]	7.176×10^{-5}	5.739×10^{-7}
Minimum of $F_R _{dB}$ [dB]	-82.88	-124.82
Maximum of $F_R _{lin}$ [V/m]	1.309×10^{-4}	2.343×10^{-5}
Maximum of $F_R _{dB}$ [dB]	-77.66	-92.60
Average $F_R _{lin}$ [V/m]	1.112×10^{-4}	1.230×10^{-5}
Average $F_R _{dB}$ [dB]	-79.08	-98.20
Variance	2.403×10^{-10}	4.005×10^{-11}

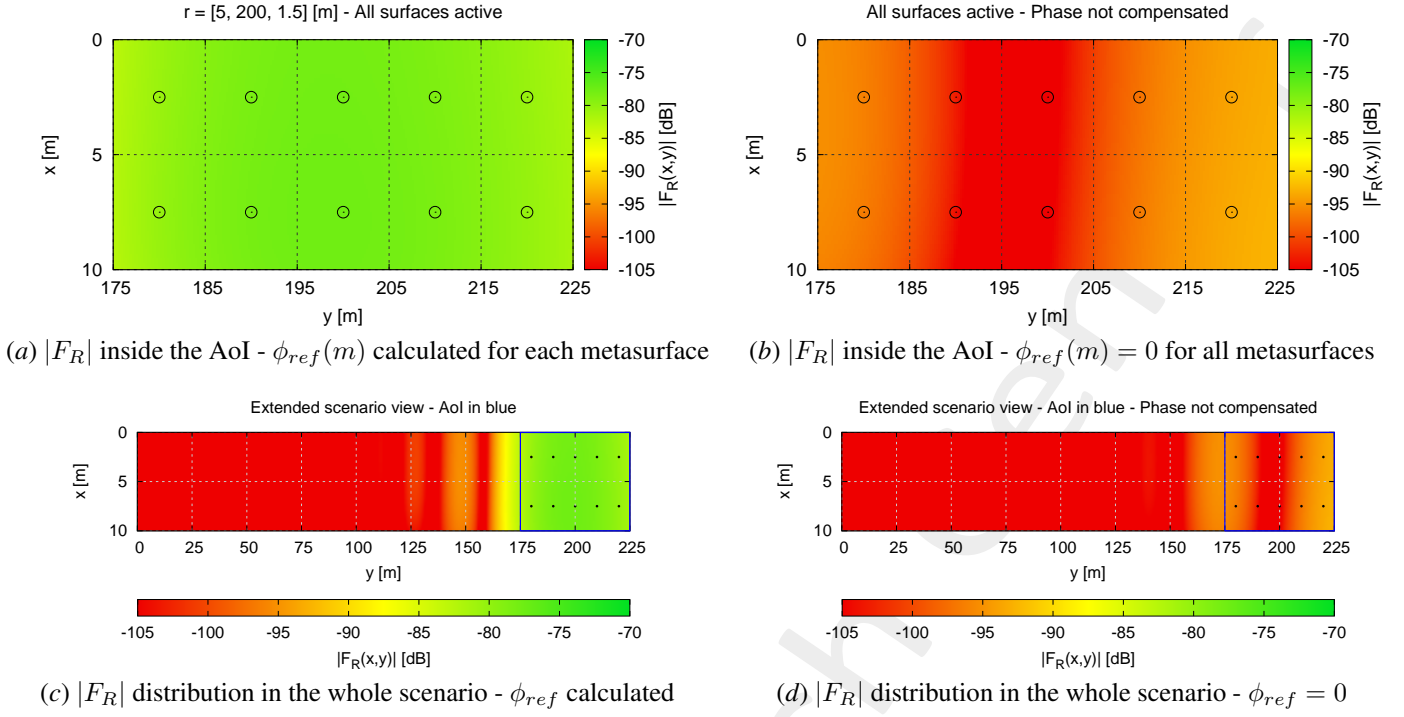


Figure 8: Influence of phase term $\phi_{ref}(m)$ on the final value of the total field F_R , with m indicating the surface ID

1.3 The Optimization

The formulated problem considers the effect that the contributions of the single metasurfaces have on the overall received field inside an area of blind spot, referred to as area of interest (AoI). In this optics, it is possible to consider the problem as a multi-dimensional binary problem, in which the variables are binary and correspond to the status of each individual surface that composes the smart skin (present or absent - ON or OFF). In order to try and find the most suitable solutions for it, the problem has been reformulated as an optimization problem, in which the objective would be achieving the maximum quality of the signal in the region while keeping limited the amount of metasurfaces employed. The number of variables of this problem is therefore the maximum number of metasurfaces that are considered for each scenario, and the optimal solution would not be singular, but it would instead form a “Pareto front” of trade-off solutions, as it is the case with conflicting cost functions. The choice of which of the solutions on the Pareto front to use shall be performed at a later stage according to the needs and objective of the final real-life deployment.

To perform the optimization, the optimizer ESPRESSO, an optimization platform made available by *Eledia@UniTN*, has been employed, setting it to function with a NSGA-II (Nondominated-Sorting Genetic Algorithm II) algorithm, as reported in the following subsection.

Naturally, there are many other degrees of freedom in the system, on which it is possible to define different optimization objectives or variables, so the present work has to be considered as a “first step” towards a more complete and complex analysis of a scenario whose importance will surely increase with the growth of future-generation communication standards.

1.3.1 The NSGA-II algorithm

As mentioned, the problem, as it is considered, is in its nature a binary problem. Because of this, the optimization algorithm chosen to be paired with the simulation software described above was a Genetic Algorithm (GA). A Genetic Algorithm is a sub-set of Evolutionary Algorithms, optimization techniques whose main advantages consist of their robustness in achieving a global solution, the easiness in the definition of the working frame, objectives and variables, and the vast amount of literature to back them up. In particular, Genetic Algorithm fits well with binary problems thanks to the concept of crossover and the implicit parallelization of the optimization process that it implies.

As the problem is formulated as a multi-objective optimization, a multi-objective algorithm was needed, and, between the algorithms implemented in ESPRESSO, the NSGA-II (Nondominated-Sorting Genetic Algorithm II) was chosen as the best fit to work with a multiple objective binary problem, as in the case of the defined scenario.

For the implementation of the EM smart skin optimization, the parameters of the NSGA-II algorithm have been set as follows:

- Population dimension: $2 \times N_{tot}$ individuals, where N_{tot} is the number of variables (i.e., the maximum number of metasurfaces that can compose the smart skin)
- Number of iterations: 1000
- Cross-over rate: 1.0
- Cross-over distribution: 15.0
- Mutation rate: $\frac{1}{N_{tot}}$
- Mutation distribution: 20.0

To increase its statistical relevance, the simulation has been validated considering a wide set of different random seeds, with minimal differences between their respective results.

1.3.2 Cost function definition

As already mentioned, the two conflicting properties that were considered for the optimization are the coverage satisfaction and the system complexity. The mathematical formulation of these two cost functions is hereby reported:

$$\Phi_1(\underline{r}, \underline{a}) = \frac{1}{M} \cdot \sum_{m=1}^M \frac{||E_{tot}(\underline{r}_m, \underline{a})||_{dB} - E_{th}|_{dB}}{|E_{th}|_{dB}} \cdot H[E_{th}|_{dB} - |E_{tot}(\underline{r}_m, \underline{a})|] \quad (4)$$

$$\Phi_2(N_{active}) = \frac{N_{active}}{N_{tot}} \quad (5)$$

where:

- M is the total number of observation points in the scenario, where the m -th observer has coordinates defined by $\underline{r}_m \in \mathbb{R}^3$;

- $E_{tot}(\underline{r}_m, \underline{a})$ is the total field calculated at the observation point \underline{r}_m of the scenario, which depends on the vector of boolean variables \underline{a} of length N_{tot} that defines if the n -th surface is active ($a(n) = 1$) or not ($a(n) = 0$);
- E_{th} is the threshold value for the field that the optimizer aims at achieving as the lowest acceptable value, set to -70 [dB] for the simulations, as a reasonable electric field level to consider an area as “good coverage” in a real-life scenario;
- $H[E_{th}|_{dB} - |E_{tot}(\underline{r}_m, \underline{a})|]$ is the Heaviside step function defined as: The meaning of this function is that only the cases in which the received field is lower than the threshold value are considered for the optimization;
- N_{active} is the number of surfaces considered present in a given optimization iteration;
- N_{tot} is the total number of metasurfaces that can be present, i.e., the maximum number of positions on which metasurfaces can be installed in a given scenario.

For both cost functions, the algorithm was asked to perform a minimization.

The meaning of the two cost functions, as derives from the mathematical formulation, can be explained as follows:

1. Φ_1 , the “coverage satisfaction” (Eq. 4), is a formulation commonly used in the telecommunication field to assess the quality of the received signal and the power of the electromagnetic field at different points of observation, as it evaluates how far below the satisfactory threshold E_{th} the observers are;
2. Φ_2 , the “complexity” (Eq. 5), is a straightforward expression of the complexity of the smart skin deployment, as it indicates which percentage of the total available surfaces is actually active or present.

As it can be easily noticed, the two cost functions are by definition conflicting, as a larger number of metasurfaces would lead to a stronger electric field in reception, and vice versa. The consequence of this is that the final results of the optimization will create a Pareto front of many optimal solutions, where each of them is a valid trade-off to be considered for the final, real-life implementation of the system.

More information on the topics of this document can be found in the following list of references.

References

- [1] Benoni, F. Capra, M. Salucci, and A. Massa, "Towards real-world indoor smart electromagnetic environments - A large-scale experimental demonstration," *IEEE Trans. Antennas Propag.*, vol. 71, no. 11, pp. 8450-8463, Nov. 2023 (DOI: 10.1109/TAP.2023.3305053).
- [2] G. Oliveri, M. Salucci, and A. Massa, "Features and potentialities of static passive EM skins for NLOS specular wireless links," *IEEE Trans. Antennas Propag.*, vol. 71, no. 10, pp. 8048-8060, Oct. 2023 (DOI: 10.1109/TAP.2023.3301654).
- [3] G. Oliveri, M. Salucci, and A. Massa, "Generalized analysis and unified design of EM skins," *IEEE Trans. Antennas Propag.*, vol. 71, no. 8, pp. 6579-6592, Aug. 2023 (DOI: 10.1109/TAP.2023.3281073).
- [4] M. Salucci and A. Massa, "Unconventional sources for smart EM environments: An inverse scattering vision," *Reviews of Electromagnetics*, Invited Paper, vol 1, pp. 17-18, 2022 (DOI: 10.1109/MOCAS52088.2021.9493390).
- [5] M. Salucci, A. Benoni, G. Oliveri, P. Rocca, B. Li, and A. Massa, "A multihop strategy for the planning of EM skins in a smart electromagnetic environment," *IEEE Trans. Antennas Propag.*, vol. 71, no. 3, pp. 2758-2767, Mar. 2023 (DOI: 10.1109/TAP.2022.3233714).
- [6] G. Oliveri, F. Zardi, P. Rocca, M. Salucci, and A. Massa, "Constrained-design of passive static EM skins," *IEEE Trans. Antennas Propag.*, vol. 71, no. 2, pp. 1528-1538, Feb. 2023 (DOI: 10.1109/TAP.2022.3225593).
- [7] G. Oliveri, P. Rocca, M. Salucci, D. Erricolo, and A. Massa, "Multi-scale single-bit RP-EMS synthesis for advanced propagation manipulation through system-by-design," *IEEE Trans. Antennas Propag.*, vol. 70, no. 10, pp. 8809-8824, Oct. 2022 (DOI: 10.1109/TAP.2022.3201700).
- [8] A. Benoni, M. Salucci, G. Oliveri, P. Rocca, B. Li, and A. Massa, "Planning of EM skins for improved quality-of-service in urban areas," *IEEE Trans. Antennas Propag. - Special Issue on 'Smart Electromagnetic Environment'*, vol. 70, no. 10, pp. 8849-8862, Oct. 2022 (DOI: 10.1109/TAP.2022.3177284).
- [9] G. Oliveri, F. Zardi, P. Rocca, M. Salucci, and A. Massa, "Building a smart EM environment - AI-Enhanced aperiodic micro-scale design of passive EM skins," *IEEE Trans. Antennas Propag. - Special Issue on 'Smart Electromagnetic Environment'*, vol. 70, no. 10, pp. 8757-8770, Oct. 2022 (DOI: 10.1109/TAP.2022.3151354).
- [10] P. Rocca, P. Da RÙ, N. Anselmi, M. Salucci, G. Oliveri, D. Erricolo, and A. Massa, "On the design of modular reflecting EM skins for enhanced urban wireless coverage," *IEEE Trans. Antennas Propag. - Special Issue on 'Smart Electromagnetic Environment'*, vol. 70, no. 10, pp. 8771-8784, Oct. 2022 (DOI: 10.1109/TAP.2022.3146870).
- [11] G. Oliveri, P. Rocca, M. Salucci, and A. Massa, "Holographic smart EM skins for advanced beam power shaping in next generation wireless environments," *IEEE J. Multiscale Multiphys. Comput. Tech.*, vol. 6, pp. 171-182, Oct. 2021 (DOI: 10.1109/JMMCT.2021.3121300).

-
- [12] A. Massa, A. Benoni, P. Da RÙ, S. K. Goudos, B. Li, G. Oliveri, A. Polo, P. Rocca, and M. Salucci, "Designing smart electromagnetic environments for next-generation wireless communications," *Telecom*, Invited Paper, vol. 2, pp. 213-221, 2021 (DOI: 10.3390/telecom2020014).

ELEDIA Research Center